

PRACTICAL CASE

Phenological characterization of *Fagus sylvatica* L. in Mediterranean populations of the Spanish Central Range with Landsat OLI/ETM+ and Sentinel-2A/B

Gómez, C. ¹, Alejandro, P. ², Montes, F. ¹

¹ INIA-CIFOR, Dep. of Forest Dynamics and Management, Ctra. La Coruña km 7.5, 28040 Madrid, Spain.

² Quasar Science Resources, Ctra. La Coruña km 22.3, Las Rozas, 28232 Madrid, Spain.

Abstract: The Spanish Central Range hosts some of the southernmost populations of *Fagus sylvatica* L. (European beech). Recent cartography indicates that these populations are expanding, going up-streams and gaining ground to oak forests of *Quercus pyrenaica* Willd., heather-lands, and pine plantations. Understanding the spectral phenology of European beech populations—which leaf flush occurs earlier than other vegetation formations—in this Mediterranean mountain range will provide insights of the species recent dynamics, and will enable modelling its performance under future climate oscillations. Intra-annual series of 211 Landsat OLI/ETM+ images, acquired between April 2013-December 2019, and 217 Sentinel-2A/B images, acquired between April 2017-December 2019, were employed to characterize the spectral phenology of European beech populations and five other vegetation types for comparison in an area of 108 000 ha. Vegetation indices (VI) including the Normalized Difference Vegetation Index (NDVI) and Tasseled Cap Angle (TCA) from Landsat, and the NDVI and Enhanced Vegetation Index (EVI) from Sentinel-2 were retrieved from sample pixels. The temporal series of these VI were modelled with Savitzky-Golay and double logistic functions, and assessed with TIMESAT software, enabling the parametric characterization of European beech spectral phenology in the area with the start, length, and end of season, as well as peak time and value. The length of beech phenological season was similar when portrayed by Landsat and Sentinel-2 NDVI time series (214 and 211 days on average for the common period 2017-2019) although start and end differed. Compared with NDVI counterparts the TCA season started and peaked later, and the EVI season was shorter. Sentinel-2 NDVI peaked higher than Landsat NDVI. The European beech had an earlier (21 days on average) start of season than competing oak forests. Joint analysis of data from the virtual constellation Landsat/Sentinel-2 and calibration with field observations may enable more detailed knowledge of phenological traits at the landscape scale.

Key words: spectral phenology, European beech, Landsat, Sentinel-2, TIMESAT, NDVI, TCA, EVI.

Caracterización de la fenología de *Fagus sylvatica* L. en poblaciones mediterráneas del Sistema Central español mediante datos Landsat OLI/ETM+ y Sentinel-2A/B

Resumen: Algunas de las poblaciones más meridionales de *Fagus sylvatica* L. (haya) se encuentran en el Sistema Central español. La cartografía reciente de estas poblaciones indica que están expandiéndose a lo largo de arroyos

To cite this article: Gómez, C., Alejandro, P., Montes, F. 2020. Phenological characterization of *Fagus sylvatica* L. in Mediterranean populations of the Spanish Central Range with Landsat OLI/ETM+ and Sentinel-2A/B. *Revista de Teledetección*, 55, 71-80. <https://doi.org/10.4995/raet.2020.13561>

* Corresponding author: gomez.cristina@inia.es

y ganando terreno a robledales de *Quercus pyrenaica* Willd., brezales, y pinares. Conocer la fenología espectral de estos hayedos mediterráneos de montaña, cuya apertura de hojas se adelanta a la de otras formaciones vegetales permitiría inferir su dinámica reciente y modelizar su comportamiento frente a futuras oscilaciones climáticas. Se utilizaron 211 imágenes Landsat OLI/ETM+ adquiridas entre abril 2013-diciembre 2019 y 217 imágenes Sentinel-2A/B adquiridas entre abril 2017-diciembre 2019 para caracterizar la fenología espectral de hayedos y otras cinco formaciones vegetales en 108 000 ha. Se calcularon y analizaron índices de vegetación: *Normalized Difference Vegetation Index* (NDVI) y *Tasseled Cap Angle* (TCA) con datos Landsat, NDVI y *Enhanced Vegetation Index* (EVI) con Sentinel-2. Se extrajeron las series temporales de estos índices en píxeles muestra para analizar mediante software TIMESAT, ajustando modelos Savitzky-Golay y función logística, y describiendo paramétricamente la fenología espectral: inicio, fin, y duración de temporada, así como momento y valor máximo del índice. Las series NDVI de Landsat y Sentinel-2 representaron una duración similar de la temporada fenológica (214 y 211 días para el periodo común de análisis, 2017-2019), aunque inicio y fin no coincidieron. Comparando con las curvas NDVI homólogas, la temporada TCA comenzó y alcanzó el pico máximo antes, y la temporada EVI fue más corta. Los valores máximos de NDVI en las series Sentinel-2 fueron más altos que los de Landsat. Los hayedos comenzaron la temporada fenológica de media 21 días antes que los robledales. El análisis conjunto de datos de la constelación virtual Landsat/Sentinel-2 y la calibración con observaciones de campo permitirá conocer mejor la fenología a escala de paisaje.

Palabras clave: fenología espectral, haya, Landsat, Sentinel-2, TIMESAT, NDVI, TCA, EVI.

1. Introduction

Fagus sylvatica L. (European beech) populations in the Spanish Central Range are at the southernmost distribution limit of the species (Sánchez de Dios et al., 2016). European beech is a temperate, shade tolerant broadleaved species widely spread in Europe, mainly within the circumboreal region (Fang and Lechowicz, 2006). European beech (hereafter beech) has high water requirements, and its Mediterranean distribution is limited by summer temperatures, drought, and moisture availability (Houston Durrant et al., 2016) to locations where summer stress conditions are balanced by topographic and microclimatic factors such as fogs (Delhon and Thiébaud, 2005). At mountain locations, beech stands are exposed to strong winds and late frosts that reduce tree growth and survival rates (Houston Durrant et al., 2016; Rubio-Cuadrado et al., 2018). Although the species adapts to climate variations, extreme events induce phenological anomalies damaging the expanding leaves and flowers (Augsburger, 2013). Land use change since the middle of the twentieth century—with the abandonment of historical uses like charcoal production and grazing—as well as climate variations and extremes, are the main drivers of the recent dynamics of Mediterranean beech populations (Sánchez de Dios et al., 2016).

Time series of satellite remotely sensed data facilitate monitoring of vegetation phenology (Zeng et al., 2020) and provides information of ecosystem responses to climate variability and change (Melaas et al., 2013). In comparison with more frequently used data for characterization of phenology at the landscape scale (e.g. MODIS, AVHRR), medium spatial resolution (10-30 m pixel size) data has increased capacity for interpretation of fine scale ecological phenomena (Melaas et al., 2016). The frequency of currently available Landsat and Sentinel-2 data (Li and Roy, 2017), enables phenological characterization of species at the stand and landscape scale (Stanimirova et al., 2019). Some studies have already combined data from Landsat and Sentinel-2 for phenological characterization at regional (Jönsson et al., 2018) and continental (Bolton et al., 2020) scale. Getting knowledge of the phenology of beech forests in the Spanish Central Range will contribute towards better understanding the species recent dynamics and to predict future performance under environmental change scenarios. The goal of this work is to characterize the spectral phenology of beech populations in the Spanish Central Range with images acquired by Landsat and Sentinel-2 sensors during period 2013-2019.

2. Methods

2.1. Study area

Our study focuses on a 108 000 ha area in the Spanish Central Range (Figure 1) encompassing all beech populations mapped in this region (Gómez et al., 2019). Average annual precipitation is 710 mm and average temperature ranges between 3.2 and 15 °C (Herrera et al., 2012) with two month summer drought (Gonzalo, 2010), enabling the presence of broadleaved Atlantic species (Ruiz-Labourdette et al., 2010). Beech populations are located between 1300 and 1970 m on acidic soils derived from metamorphic materials. In these mountains beech grows intermingled with Pyrenean oak forests (*Quercus pyrenaica* Willd.) or at higher altitudes defining the tree line. Holly oak (*Quercus ilex* L.) and ash (*Fraxinus*

angustifolia Vahl.) open woodlands, shrublands, and pastures are other vegetation formations present in the area. These beech forests have traditionally been managed as open woodlands for pastures, or as coppice for production of firewood and charcoal. Since ca. 1970 the Spanish Central Range beech populations are protected under protection figures such as Natural Site of National Interest in Madrid and Segovia, and Natural Park in Guadalajara (Sánchez de Dios et al., 2020) (Figure 1). Beech occupies approximately 560 ha in the Spanish Central Range, and has since 1978 to 2015 spread over 21% of its area of distribution, gaining ground to heather lands, going up streams, and intermingled in pine plantations (Gómez et al., 2019; Sánchez de Dios et al., 2020).

An early phenology of these mountain beech populations, which leaves open at the end of April or beginning of May, facilitates advantageous

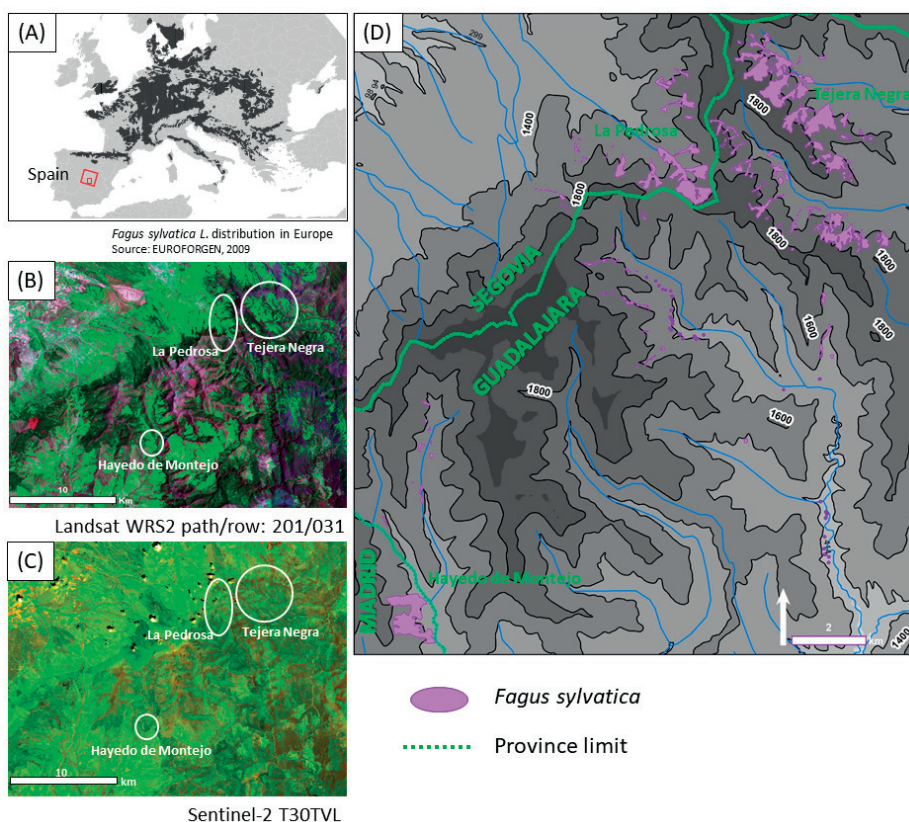


Figure 1. Study area in central Spain. (A) Overall distribution of *Fagus sylvatica* in Europe and location of study area in Spain. (B) Landsat OLI image subset with main beech populations marked. (C) Sentinel-2 image subset with main beech populations marked. (D) Distribution of beech dominated stands belonging to three Spanish provinces (Guadalajara, Segovia, Madrid).

competition over other tree species. At the same time, the early start of season exposes trees to late frosts and strong winds (Gil et al., 2010). Areas dominated by beech species had been identified and mapped through classification of multi-temporal Landsat OLI images acquired in 2015 (Gómez et al., 2019). All stands were verified through visual inspection on the ground and measurement of GPS coordinates. When access was not possible, the field observations were supported by interpretation of orthophotography.

2.2. Landsat ETM+ and OLI data

The Landsat program operated by the National Aeronautics and Space Administration (NASA) and the United States Geological Service (USGS) has currently two Landsat satellites orbiting the Earth and providing global observations at 30 m spatial resolution every 8 days (Wulder et al., 2019). Landsat 7 and 8 are equipped with the optical Enhanced Thematic Mapper Plus (ETM+) and Operational Land Imager (OLI) sensors respectively, which are fully compatible. All images acquired by the Landsat programme since 2013 are available in the USGS archive. The metadata of archived images acquired by Landsat 7 ETM+ and Landsat 8 OLI over the study area (path/row 201/031) were analysed and all images with cloud cover below 70% were considered for this study (Figure 2).

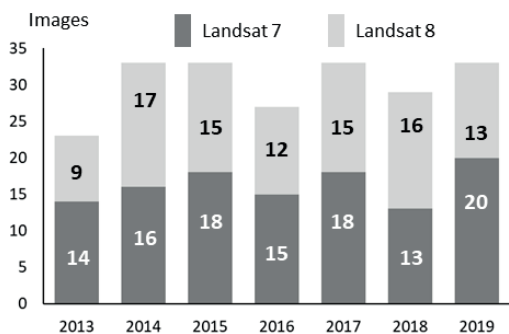


Figure 2. Landsat images (path row 201/031) with cloud coverage below 70% available in the USGS Landsat archive and used in this study.

The 211 selected Landsat images (97 ETM+ and 114 OLI) were downloaded from on-demand USGS Earth Resources Observation and Science (EROS) Center Science Processing Architecture

(ESPA) system (<https://espa.cr.usgs.gov/>) as surface reflectance (SR). Landsat images in collection 1 level 2 SR are geometrically registered and radiometrically corrected, ready for time series analysis. Clouds, shadows, and snow were masked via the quality band provided by default within the source data. Images were subset encompassing the study area (Figure 1).

2.3. Sentinel-2 data

Sentinel-2A/B is a two satellite system operated by the European Space Agency (ESA, Drusch et al., 2012). Each Sentinel-2 satellite is equipped with an optical Multi-Spectral Instrument (MSI) acquiring data at 10, 20, and 60 m spatial resolution depending on wavelength (Drusch et al., 2012). Since it became fully operational in October 2017 (Baetens et al., 2019) the dual satellite system provides observations over the study region every 2-3 days owing to the tracks' overlap at this latitude. All Sentinel-2A/B images acquired between April 2017 and December 2019 and available from <https://scihub.copernicus.eu> in level 2A format (MSIL2A) were considered for this study. Sentinel-2 MSIL2A data are atmospherically and ortho-geometrically corrected images. A few images totally covered by clouds were vetoed for further processing. A total of 217 images with T30VL spatial identifier were downloaded to disk.

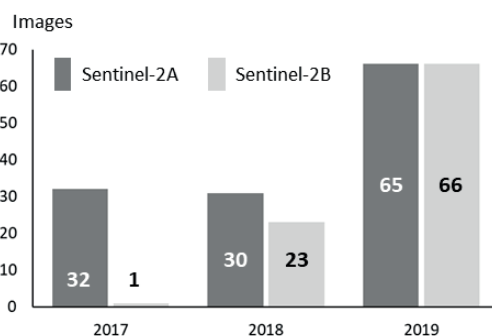


Figure 3. Sentinel-2A/B images used in the study.

The visible, NIR, and SWIR bands (2, 3, 4, 5, 6, 7, 8, 8A, 11, 12) were employed at 10 m, resampling bands 5, 6, 8A, 11, 12 and subsetting all to the area of interest in Sentinel Applications Platform (SNAP) environment. A combined mask of clouds, shadows, water, and snow was built from the scene classification source masks provided in the

MSIL2A products, buffered by an external 3 pixel window, and applied in Python environment (Van Rossum and Drake, 2009).

2.4. Vegetation indices

Some vegetation indices (VI) frequently used for phenological characterization (White et al., 2014; Zeng et al., 2019) were calculated (Table 1). We included the Tasseled Cap Angle (TCA) in our selection to test its performance for characterization of spectral phenology. For Landsat images we calculated the Normalized Difference Vegetation Index (NDVI, Tucker 1979), the Tasseled Cap Wetness (TCW, Crist, 1985) and the Tasseled Cap Angle (TCA, Powell et al., 2010). For Sentinel-2 images we calculated the NDVI, the Enhanced Vegetation Index (EVI, Liu and Huete, 1995), and the Normalized Difference Water Index (NDWI, Gao, 1996).

2.5. Spectro-phenological characterization with TIMESAT

Landsat and Sentinel-2 data series were analysed independently. Landsat observations were interpolated to 8-day and Sentinel-2 observations interpolated to 3-day series with spline functions. Values of the VI series were retrieved from samples of beech dominated stands and other five vegetation types present in the area (Gómez et al., 2019) –Pyrenean oak forests, Holly oak forests, pines, shrublands and pastures– for comparison, but we particularly focused on the contrast between beech and Pyrenean oak. The number of beech samples was 150 from a total of 262. The spatial unit for all

characterizations and analysis was the pixel. Only samples with a clear cyclic pattern of the VI time series were considered in the retrieval of phenological parameters. TIMESAT software (Eklundh and Jönsson, 2017) was employed for characterization of spectro-phenological traits. TIMESAT provides parameters such as start of season (SOS), end of season (EOS), seasonal length, and peak values. TIMESAT is robust to data noise –e.g. by residual clouds– and series incompleteness, and provides information of the results quality increasing its reliability. TIMESAT flexibility makes it well-suited for characterization of regional phenology (Stanimirova et al., 2019). The SOS and EOS parameters were determined based on seasonal amplitude, defined as the interval between the base and maximum VI values for each individual season. The SOS occurs when the left part of the fitted curve reaches 0.5 that amplitude value, counted from the base level, and the end of season is defined similarly but for the right side of the curve. Since field observations were not available for calibration of TIMESAT parameters, default values were set up, with one season per year. Savitzky-Golay filters and double logistic models were fitted to individual series (Eklundh and Jönsson, 2017; Stanimirova et al., 2019).

3. Results

Double logistic functions generalize phenological curves and are adequate for characterization of overall patterns, whereas Savitzky-Golay filters more smoothly follow seasonal variations, enabling identification of punctual anomalies (Figure 4).

Table 1. Vegetation indices used to characterize phenological traits in other studies.

	Equation	Reference
Landsat and Sentinel-2	$NDVI = (NIR - Red) / (NIR + Red)$	Tucker, 1979
Landsat	$TCW = 0.0315 \times Blue + 0.2021 \times Green + 0.3102 \times Red + 0.1594 \times NIR + 0.6806 \times SWIR1 - 0.6109 \times SWIR2$	Crist, 1985
Landsat	$TCA = \text{atan}(TCG/TCB)$ $TCB = 0.2043 \times Blue + 0.4158 \times Green + 0.5524 \times Red + 0.5741 \times NIR + 0.3124 \times SWIR1 + 0.2303 \times SWIR2$ $TCG = -0.1603 \times Blue - 0.2819 \times Green - 0.4934 \times Red + 0.7940 \times NIR + 0.0002 \times SWIR1 - 0.1446 \times SWIR2$	Powell et al., 2010
Sentinel-2	$EVI = 2.5 \times [(NIR - Red) / (NIR + 6 \times Red - 7.5 \times Blue + 1)]$	Liu and Huete, 1995
Sentinel-2	$NDWI = (NIR - SWIR3) / (NIR + SWIR3)$	Gao, 1996

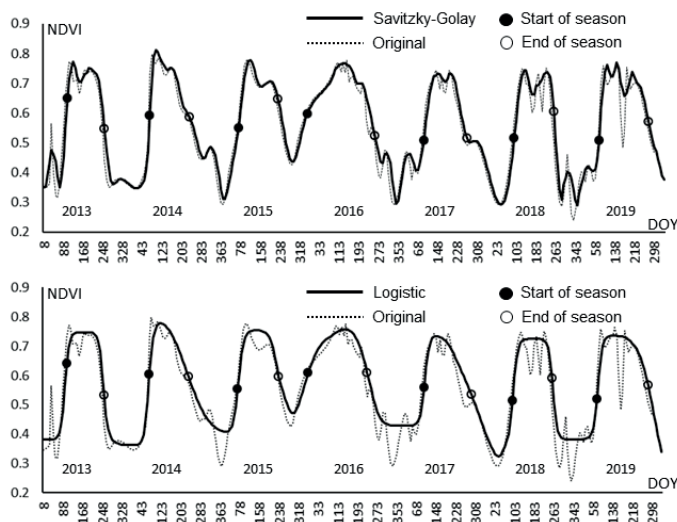


Figure 4. Representation of a modelled phenological curve of *Fagus sylvatica* with Savitzky-Golay filter (top) and double logistic function (bottom).

NDVI and TCA time series of all samples portrayed clearly cyclic patterns representing phenological seasons. Some samples did not show a clear cyclic pattern of the EVI time series and we selected 35% of them to consider in the retrieval of phenological parameters. Time series of wetness indices (TCW in Landsat and NDWI in Sentinel-2) were also noisier and less convenient for retrieval of phenological information.

3.1. Spectral phenology with Landsat ETM+ and OLI

The Landsat NDVI series fitted with Savitzky-Golay and double logistic functions indicate that during the period analysed with Landsat data (2013-2019) beech SOS was DOY (day of year)

122 on average and beech EOS was DOY 336. On average the length of phenological season was 214 days and it peaked DOY 226. Time series analysis with TIMESAT showed that beech phenology characterized with the TCA is shorter than with NDVI (7 days on average for period 2013-2019), as it starts and peaks later (6 and 4 days on average, respectively) but on average ends just one day later (Table 2).

During the period analysed with Landsat data (2013-2019) beech dominated areas started the phenological season on average 16 days earlier than Pyrenean oak stands (Figure 5) but the EOS coincided. Beech spectro-phenological seasons were therefore on average 17 days longer than Pyrenean oak counterparts.

Table 2. Resume of phenological parameters obtained from Landsat time series with TIMESAT. SOS, EOS, length and peak parameters average results of Savitzky-Golay and double logistic functions.

	SOS (DOY)		EOS (DOY)		Length (days)		Peak (DOY)	
	NDVI	TCA	NDVI	TCA	NDVI	TCA	NDVI	TCA
2013	138	142	344	336	206	194	245	244
2014	124	127	336	337	212	210	221	222
2015	125	125	317	312	191	188	217	217
2016	80	87	326	329	246	242	197	205
2017	118	131	348	349	231	219	228	235
2018	136	144	331	332	195	187	235	242
2019	130	139	350	349	220	210	240	248
Average	122	128	336	335	214	207	226	230

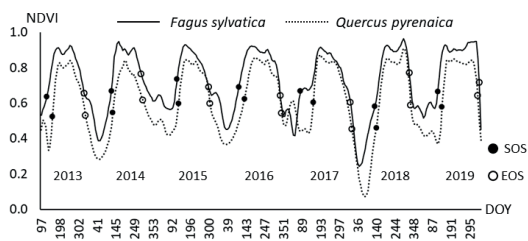


Figure 5. Spectral phenology of *Fagus sylvatica* and *Quercus pyrenaica* samples portrayed with a Savitzky-Golay function adjusted to Landsat NDVI series.

3.2. Spectral phenology with Sentinel-2

Although the three-season period analysed (2017-2019) is short to reliably average phenological parameters –especially because year 2017 registered a relevant late frost between 26th and 28th of April– Sentinel-2 series fitted with Savitzky-Golay and double logistic functions indicate similar patterns. There is apparently a trend towards earlier SOS, EOS and peak time. The beech average SOS portrayed by NDVI was DOY 97, average EOS was DOY 308, and average length of season 211 days. Interestingly, despite the late SOS in 2017, that year the spectro-phenological season was five days longer than average due to its late EOS. Compared with the NDVI phenology, EVI showed a 9-day later SOS on average and considerably shorter length of season (33 days shorter on average).

According to the NDVI series analysed with TIMESAT, areas dominated by beech had on average a 6-day earlier SOS than areas dominated by oak. Some of the NDVI series show the effect of the 2017 late frost by a marked minimum (Figure 6). This event affected samples with irregular variations of SOS. On average, beech EOS during period 2017-2019 was 24 days later

than Pyrenean oak EOS. Beech season length was on average 30 days longer and it peaked 4 days later on average.

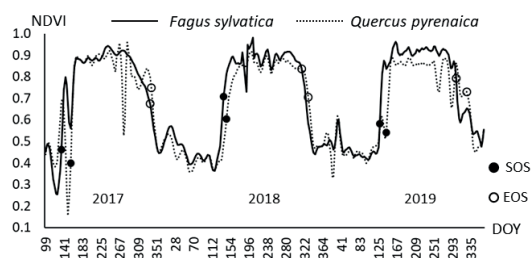


Figure 6. Spectral phenology of *Fagus sylvatica* and *Quercus pyrenaica* samples portrayed with a Savitzky-Golay function adjusted to Sentinel-2 NDVI series.

4. Discussion and Conclusions

Intra-annual series of medium spatial resolution data from Landsat and Sentinel-2 enables characterization of spectral phenology of ecosystems and individual dominant species like *Fagus sylvatica* L. populations in the Spanish Central Range. Although the presence of clouds results in some time intervals lacking good quality observations, the improved frequency of data acquired by both programs provides valuable insights of spectral phenology. Joint analysis of the virtual constellation data may be needed if higher frequency of clouds are present. Likewise, a longer period of data would improve the insights, enabling observation of changing trends (e.g. Bucha and Koren, 2017).

Despite differences in determination of phenological parameters such as SOS and EOS due to temporal frequency differences, the same patterns were observed by both Landsat and Sentinel-2 intra-annual series. Furthermore, interannual comparison of consistent estimations provides accurate assessments of changes in phenology over

Table 3. Resume of phenological parameters obtained from Sentinel-2 NDVI and EVI time series with TIMESAT. SOS, EOS, length and peak parameters average results of Savitzky-Golay and double logistic functions.

	SOS (DOY)		EOS (DOY)		Length (days)		Peak (DOY)	
	NDVI	EVI	NDVI	EVI	NDVI	EVI	NDVI	EVI
2017	103	119	323	297	220	178	208	205
2018	99	104	312	274	213	169	199	189
2019	90	97	289	284	199	187	186	190
Average	97	107	308	285	211	178	198	195

time, and may contribute to better understanding the adaptation of species to environmental conditions (Dittmar and Elling, 2006) and change.

NDVI has been frequently used for assessment of spectral phenology (e.g. Fu et al., 2014; Gerard et al., 2020), and was in our study the most reliable VI across sensors for characterization of phenological traits. The Landsat Tasseled Cap Transformation derived TCA performed similarly and portrayed shorter and delayed seasons. EVI and the wetness VI essayed here (TCW for Landsat and NDWI for Sentinel-2) were noisier and less reliable for characterization of phenological traits.

Time series analysis with TIMESAT enabled verification of the unique character of beech dominated areas comparing phenological parameters in different vegetation formations. *Fagus sylvatica* season starts consistently earlier and it is longer than *Quercus pyrenaica* season in the Spanish Central Range, which may confer it a competitive advantage.

Acknowledgments

This work was funded by the Spanish Ministry of Science, Innovation and University through projects: AGL2013-46028-R “Forest management facing the change in forest ecosystems dynamics: a multiscale approach (SCALyFOR)” and AGL201676769-C2-1-R “Influence of natural disturbance regimes and management on forests dynamics, structure and carbon balance (FORESTCHANGE)”. Field work assistance by Diego Galán, Belén Oñate, and Gregorio Cerezo, and the support of José Juárez Benítez, director of the Sierra Norte de Guadalajara Natural Park are much appreciated.

References

Augspurger, C.K. 2013. Reconstructing patterns of temperature, phenology, and frost damage over 124 years: Spring damage risk is increasing. *Ecology* 94, 41-50. <https://doi.org/10.1890/12-0200.1>

Bolton, D.K., Gray, J.M., Melaas, E.K., Moon, M., Eklundh, L., Friedl, M.A. 2020. Continental-scale land surface phenology from harmonized Landsat 8 and Sentinel-2 imagery, *Remote Sensing of Environment*, 240, 111685. <https://doi.org/10.1016/j.rse.2020.111685>

Bucha T, Koren, M. 2017. Phenology of the beech forests in the Western Carpathians from MODIS for 2000-2015. *iForest (Biosciences and Forestry)*, 10, 537-546. <https://doi.org/10.3832/ifor2062-010>

Crist, E.P. 1985. A TM Tasseled Cap equivalent transformation for reflectance factor data. *Remote Sensing of Environment*, 17, 301-306. [https://doi.org/10.1016/0034-4257\(85\)90102-6](https://doi.org/10.1016/0034-4257(85)90102-6)

Delhon, C., Thiébaud, S. 2005. The migration of beech (*Fagus sylvatica* L.) up the Rhone: the Mediterranean history of a “mountain” species. *Veget. Hist. Archaeobot.*, 14, 119-132. <https://doi.org/10.1007/s00334-005-0068-9>

Dittmar, C., Elling, W. 2006. Phenological phases of common beech (*Fagus sylvatica* L.) and their dependence on region and altitude in Southern Germany. *European Journal of Forest Research*, 125, 181-188. <https://doi.org/10.1007/s10342-005-0099-x>

Drusch, M., Del Bello, U., Carlier, S., Colin, O., Fernández, V., Gascon, F., Hoersch, B., Isola, C., Labertini, P., Marimort, P., Meygret, A., Spoto, F., Sya, O., Marchese, F., Bargellini, P. 2012. Sentinel-2: ESA's optical high-resolution mission for GMES operational services. *Remote Sensing of Environment*, 120, 25-36. <https://doi.org/10.1016/j.rse.2011.11.026>

Eklundh, L., Jönsson, P. 2017. Timesat 3.3 Software Manual, Lund and Malmö University, Sweden.

Fang, J., Lechowicz, M.J. 2006. Climatic limits for the present distribution of beech (*Fagus* L.) species in the world. *Journal of Biogeography*, 33, 1804-1819. <https://doi.org/10.1111/j.1365-2699.2006.01533.x>

Fu, Y.H., Piao S., Op de Beeck, M.O., Cong, N., Zhao, H., Zhang, Y., Menzel, A., Janssens, I.A., 2014. Recent spring phenology shifts in western Central Europe based on multiscale observations. *Global Ecology and Biogeography*, 23(11), 1255-1263. <https://doi.org/10.1111/geb.12210>

Gerard F.F., George, C.T., Hayman, G., Chavana-Bryant, C., Weedon, G.P. 2020. Leaf phenology amplitude derived from MODIS NDVI and EVI: maps of leaf phenology synchrony for Meso- and South America. *Geosciences Data Journal*, 00, 1–14. <https://doi.org/10.1002/gdj3.87>

Gao, B.C. 1996. NDWI—A normalized difference water index for remote sensing of vegetation liquid water from space. *Remote Sensing of Environment*, 58(3), 257-266. [https://doi.org/10.1016/S0034-4257\(96\)00067-3](https://doi.org/10.1016/S0034-4257(96)00067-3)

- Gil, L., Náger, J.A., Aranda-García, I., González-Doncel, I., Gonzalo-Jiménez, J., López de Heredia, U., Millerón, M., Nanos, N., Perea García-Calvo, R., Rodríguez-Calcerrada, J., Valbuena-Carabaña, M. 2010. *El Hayedo de Montejo: una gestión sostenible*. Dirección General del Medio Ambiente, Spain, 151 pp.
- Gómez, C., Alejandro, P., Aulló-Maestro, I., Hernández, L., Sánchez de Dios, R., Sainz-Ollero, H., Velázquez, J.C., Montes, F. 2019. Presence of European beech in its Spanish southernmost limit characterized with Landsat intra-annual time series. *Proceedings of the AIT 2018, IX Conference of the Italian Society of Remote Sensing*.
- Gonzalo, J. 2010. *Diagnosis fitoclimática de la España peninsular. Hacia un modelo de clasificación funcional de la vegetación y de los ecosistemas peninsulares españoles*. Serie Técnica: Naturaleza y Parques Nacionales. Ministerio de Medio Ambiente y Medio Rural y Marino. Organismo Autónomo Parques Nacionales.
- Herrera, S., Gutiérrez, J.M., Ancell, R., Pons, M.R., Frías, M.D., Fernández, J. 2012. Development and Analysis of a 50 year high-resolution daily gridded precipitation dataset over Spain (Spain02). *International Journal of Climatology*, 32, 74-85. <https://doi.org/10.1002/joc.2256>
- Houston Durrant, T., de Rigo, D., Candullo, G. 2016. *Fagus sylvatica* and other beeches in Europe: distribution, habitat, usage and threats in San Miguel Ayanz, J., de Rigo, D., Candullo, G., Houston Durrant, T., Mauri, A. (eds.) *European Atlas of Forest Tree Species*. Publication Office of the European Union, Luxembourg, pp.e012b90
- Jönsson, P., Cai, Z., Melaas, E., Friedl, M., Eklundh, L. 2018. A method for robust estimation of vegetation seasonality from Landsat and Sentinel-2 time series data. *Remote Sensing*, 10, 365. <https://doi.org/10.3390/rs10040635>
- Li, J., Roy, D.P. 2017. A global analysis of Sentinel-2A, Sentinel-2B and Landsat-8 data revisit intervals and implications for terrestrial monitoring. *Remote Sensing*, 9, 902. <https://doi.org/10.3390/rs9090902>
- Liu, H.Q., Huete, A.R. 1995. A feedback based modification of the NDVI to minimize canopy background and atmospheric noise. *IEEE Transactions on Geoscience and Remote Sensing*, 33, 457-465. <https://doi.org/10.1109/TGRS.1995.8746027>
- Melaas, E.K., Friedl, M.A., Zhu, Z. 2013. Detecting interannual variation in deciduous broadleaf forest phenology using Landsat TM/ETM+ data. *Remote Sensing of Environment*, 132, 176-185. <https://doi.org/10.1016/j.rse.2013.01.011>
- Melaas, E.K., Sulla-Menashe, D., Gray, J.M., Black, T.A., Morin, T.H., Andrew, D.R., Friedl, M.A. 2016. Multisite analysis of land surface phenology in North American temperate and boreal deciduous forests from Landsat. *Remote Sensing of Environment*, 186, 452-464. <https://doi.org/10.1016/j.rse.2016.09.014>
- Powell, S.L., Cohen, W.B., Healey, S.P., Kennedy, R.E., Moisen, G.G., Pierce, K.B., Ohmann, J.L. 2010. Quantification of live aboveground biomass dynamics with Landsat time-series and field inventory data: a comparison of empirical modeling approaches. *Remote Sensing of Environment*, 114, 1053-1068. <https://doi.org/10.1016/j.rse.2009.12.018>
- Rubio-Cuadrado, A., Camarero, J.J., Del Río, M., Sánchez-González, M., Ruiz-Peinado, R., Bravo-Oviedo, A., Gil, L., Montes, F. 2018. Long-term impacts of drought on growth and forest dynamics in a temperate beech-oak-birch forest. *Agricultural and Forest Meteorology*, 259, 48-59. <https://doi.org/10.1016/j.agrformet.2018.04.015>
- Ruiz-Labourdette, D., Nogués-Bravo, D., Sainz-Ollero, H., Schmitz, M.F., Pineda, F.D. 2012. Forest composition in Mediterranean mountains is projected to shift along the entire elevational gradient under climate change. *Journal of Biogeography*, 39, 162-176. <https://doi.org/10.1111/j.1365-2699.2011.02592.x>
- Sánchez de Dios, R., Hernández, L., Montes, F., Sainz-Ollero, H., Cañellas, I. 2016. Tracking the leading edge of *Fagus sylvatica* in North-Western Iberia: Holocene migration inertia, forest succession and recent global change. *Perspectives in Plant Ecology, Evolution and Systematics*, 20, 11-21. <https://doi.org/10.1016/j.ppees.2016.03.001>
- Sánchez de Dios, R., Gómez, C., Aulló, I., Cañellas, I., Gea-Izquierdo, G., Montes, F., Sainz-Ollero, H., Velázquez, J.C., Hernández, L. 2020. *Fagus sylvatica* L. peripheral populations in the Mediterranean Iberian Peninsula: climatic or anthropic relicts? *Ecosystems*. <https://doi.org/10.1007/s10021-020-00513-8>
- Stanimirova, R., Cai, Z., Melaas, E.K., Gray, J.M., Eklundh, L., Jönsson, P., Friedl, M.A. 2019. An empirical assessment of the MODIS land cover dynamics and TIMESAT land surface phenology algorithms. *Remote Sensing*, 11, 2201. <https://doi.org/10.3390/rs11192201>
- Tucker, C.J. 1979. Red and photographic infrared linear combinations for monitoring vegetation. *Remote Sensing of Environment*, 8(2), 127-150. [https://doi.org/10.1016/0034-4257\(79\)90013-0](https://doi.org/10.1016/0034-4257(79)90013-0)

Van Rossum, G., Drake, F.L., 2009. *Python 3 reference manual*. Soho Books. Scotts Valley, CA, USA. 244 pp.

Wulder, M.A., et al. 2019. Current status of Landsat program, science, and applications. *Remote Sensing of Environment*, 225, 127-147. <https://doi.org/10.1016/j.rse.2019.02.015>

Zeng, L., Wardlow B.D., Xiang, D., Hu, S., Li, D. 2020. A review of phenological metrics extraction using time-series, multispectral data. *Remote Sensing of Environment*, 237, 111511. <https://doi.org/10.1016/j.rse.2019.111511>